Intrinsic Rate Constants k_{et} of Photoinduced Electron Transfer between Anthracene Derivatives and Aromatic Donors: Does the Intersecting-State Model Challenge *Marcus* Theory When Confronted with an Archetypal Set of Data?

by **Manuel Dossot** and **Patrice Jacques***

Department of Photochemistry, Université de Haute Alsace 3, rue Alfred Werner, F-68093 Mulhouse Cedex (Phone: +33-3-89-33-68-28; e-mail: p.jacques@uha.fr)

Dedicated to Professor *André M. Braun* on the occasion of his 60th birthday

Intrinsic photoinduced electron transfer (PET) rate constants k_{et}, resorting to classically studied acceptor-donor couples, are confronted to two theoretical models of electron transfer. At a very exergonic driving force, k_{et} remains on a plateau value centered around 10^{11} s^{-1}. It is shown that the well-known and widely used *Marcus* theory fails to account for the data located on this plateau. On the contrary, the basically different approach of the intersecting-state model (ISM) allows fitting the whole set of data with physically realistic parameters. The possibility is discussed that this success of the ISM over the *Marcus* model may give hints to explain the lack of an inverted region in forward PET in solution.

Introduction. – Since the pioneering work of *Rehm* and *Weller* [1], numerous experimental data have been collected that deal with bimolecular photoinduced electron transfer (PET) in solution. In most of the studies, the bimolecular quenching rate constants k_Q are reported, obtained from conventional *Stern-Volmer* plots. When the driving force ΔG_{et} becomes sufficiently negative, k_Q is diffusion-controlled. To extract the forward electron-transfer rate constants k_{et}, a kinetic scheme including the diffusion step should be postulated [1]. By contrast, one elegant manner to circumvent the restrictive effect of diffusion is to use the so-called transient effect, observed at high concentrations of quencher [2–5]. Applying an adequate theoretical treatment to this effect enables one to obtain both the electron-transfer distance r_{et} and the true rate constant k_{et}. Such an approach has been applied in previous work to very archetypal acceptor/donor couples: anthracene derivatives as acceptors and aromatic electron donors [5]. These systems can be considered models for PET, and, *e.g.*, have been used to clearly demonstrate the existence of the inverted region in back electron transfer within geminate ion pairs [6][7]. However, in *forward* PET it is quite surprising that the same systems have not shown an inverted region. Concerning these previous results [5], it was shown that when plotting $\log k_{et}$ *vs.* ΔG_{et}, all the data followed the same trend. Namely, k_{et} started to increase rapidly when ΔG_{et} became negative, until a plateau was reached. As ΔG_{et} became more exergonic, k_{et} remained on this plateau, which could not be attributed to the classical limit of diffusion since by virtue of the transient effect, the *intrinsic* rate constant k_{et} was measured. The latter leveled off around $1.7 \cdot 10^{11}$ s^{-1}, which was one order of magnitude too low to correspond to

solvent-controlled adiabatic behavior [5a]. Although predicted by the widely used *Marcus* theory of electron transfer, the famous inverted region was not observed. This surprising finding was at this time tentatively explained by rotational orientation effects [5a]. However, some new theoretical considerations on electron transfer, based on the intersecting-state model (ISM), have arisen these latter years [8], which might be useful in giving some new insights into this unexpected non-diffusional plateau. As the examples of *Marcus* inverted regions in forward bimolecular photoinduced electron transfers are very scarce and debatable [9], the existence of this plateau, if not an artifact, could be particularly important to explain the origin of this deficiency. Consequently, in this paper, the two antagonistic theoretical conceptions of electron transfer, the *Marcus* model and ISM, will be confronted to the previously collected data to examine the physical meaning of the intrinsic plateau of k_{et} values.

Results. – *Preamble.* In *Table 1*, the experimental values of k_{et} previously determined by transient-effect analysis are collected for three anthracene acceptors and various aromatic donors in MeCN [5a]. These values were derived from the study of stationary fluorescence at high quencher concentrations. The non-*Stern-Volmer* plots

Table 1. *Free Enthalpy and Intrinsic Rate Constants of Electron Transfer in Acetonitrile for the Different Acceptor/Donor Couples*

Acceptor	Donor	ΔG_{et} [eV][a])	log k_{et}
Anthracene-9,10-dicarbonitrile	tmbd[b])	– 1.82	11.2
	dmbd[c])	– 1.59	11.2
	4-methylbenzenamine	– 1.18	11.3
	N,*N*-dimethylbenzenamine	– 1.18	11.2
	diphenylamine	– 1.01	11.3
	1,2,4-trimethoxybenzene	– 0.82	11.2
	1,4-dimethoxybenzene	– 0.65	11
	benzenamine	– 0.54	11.2
	1,3-dimethoxybenzene	– 0.44	10.8
	1,2-dimethoxybenzene	– 0.5	10.9
	1-methoxy-4-methylbenzene	– 0.39	10.7
Anthracene-9-carbonitrile	*N*,*N*-dimethylbenzenamine	– 0.84	11.3
	diphenylamine	– 0.67	11.4
	1,2,4-trimethoxybenzene	– 0.48	11.1
	1,4-dimethoxybenzene	– 0.31	10.1
	1,3-dimethoxybenzene	– 0.1	9.4
	1,2-dimethoxybenzene	– 0.16	10
	hexamethylbenzene	– 0.02	9.2
	1-methoxybenzene	0.14	6.6
Anthracene	*N*,*N*-dimethylbenzenamine	– 0.52	10.9
	1,2,4-trimethoxybenzene	– 0.16	10.3
	1,4-dimethoxybenzene	0.01	9.3
	1,3-dimethoxybenzene	0.22	7.6
	1,2-dimethoxybenzene	0.16	7.9

[a]) Calculated from the *Rehm-Weller* relationship [1] with no coulombic interaction and requisite properties of molecules given in [5a] and [10]. b) tmbd = *N*,*N*,*N*′,*N*′-Tetramethylbenzene-1,4-diamine (formerly called TMPD). [c]) dmbd = *N*,*N*-Dimethylbenzene-1,4-diamine (formerly called DMPD).

were analyzed with equations of the finite sink model [5a][4]. From the previous data, those were extracted concerning anthracene, anthracene-9-carbonitrile, and anthracene-9,10-dicarbonitrile. The few data for which exciplex formation could be suspected were excluded. In *Fig. 1*, the data of *Table 1* are plotted *vs.* the electron transfer driving force ΔG_{et}. The latter was calculated according to the well-known *Rehm-Weller* relationship [1], in which the coulombic term was not taken into account. This approximation does not much influence the result of calculation since experiments were conducted in MeCN, a polar solvent. Properties of acceptors and donors used for this calculation have been published elsewhere [5a][10]. The plateau value of k_{et} was clearly observed, even at $\Delta G_{et} = -1.9$ eV (see *Fig. 1*). Our aim was to analyze these kinetic data by the frameworks of the *Marcus* theory and ISM. Let us briefly recall the major tenants of these two antagonistic conceptions.

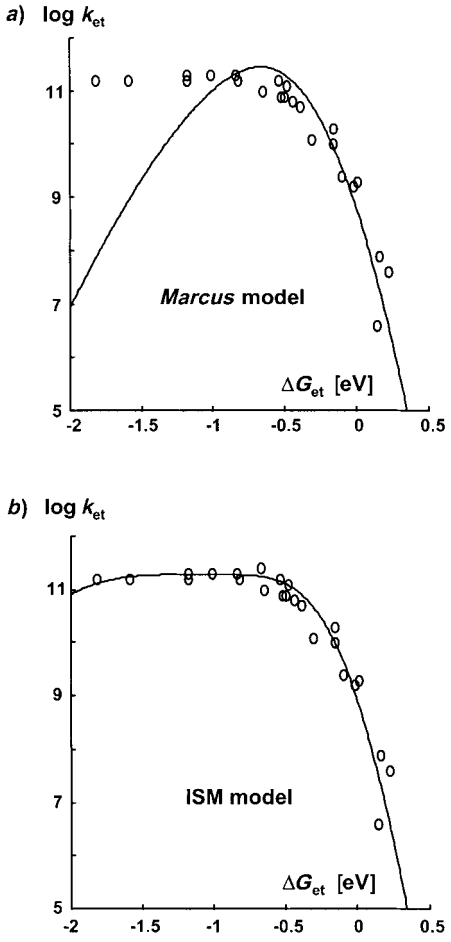

Fig. 1. *Plots of the data of* Table 1 (○) *and the best fits obtained for* a) *the* Marcus *model and* b) *the intersecting-state model, with parameters collected in* Table 2 (plain lines)

Marcus *Theory*. In *Marcus* theory [11], the potential energy of reactants and products is depicted by two parabolas of the same curvature, with the reaction coordinate on the abscissa mainly governed by the nuclear reorganization of the surrounding medium. The vertical separation of the two parabolas at the bottom of the reactants' well defines the very well-known reorganization energy λ. This term can be divided into internal reorganization λ_i, which is intrinsic of the two partners undergoing the electron transfer, and solvent reorganization λ_S. For aromatic compounds, λ_i ranges from 0.1 to 0.25 eV. Estimation of λ_S by a dielectric continuum model brings about values in the range of 0.5 – 1.5 eV in polar solvents, depending on the molecular radii of the reactants. Thus, according to *Marcus* theory, the solvent has a fundamental influence on k_{et}. These solvent fluctuations are needed to equalize the potential energy of reactants and products (crossing point of the two parabolas). At the crossing point, electron transfer between reactants can occur by classical or tunneling ways, and the system can reach the curve of products. Fundamentally, the major conception of *Marcus* originates from the fact that electron jump is such a fast process that it can be isolated from nuclear internal reorganization, respecting the *Franck-Condon* principle [11b]. The requirement of solvent fluctuations stems from the principle of energy conservation: it is fulfilled when the electron jump occurs at the crossing point, where energies of reactants and products are equal. Thus, the activation barrier almost entirely proceeds from the reorganization of the solvent cage. Quantum refinements of the theory lead to the widely used semi-empirical expression given in *Eqn. 1* [11a].

$$k_{et} = \frac{2\pi}{\hbar} H_{el}^2 \frac{1}{\sqrt{4\pi\lambda_S k_B T}} \sum_n^{\infty} \left[\frac{e^{-S} S^n}{n!} \exp\left(- \frac{(\Delta G_{et} + \lambda_S + n h\omega)^2}{4\lambda_S k_B T} \right) \right] \qquad (1)$$

In this equation, solvent reorganization modes are treated classically, and internal modes are treated by quantum mechanics. *Eqn. 1* is actually a simplification that takes into account only one average internal mode $h\omega$, but using the complete expression would not change the conclusions of this study. In *Eqn. 1*, λ is the total reorganization energy ($\lambda = \lambda_S + \lambda_i$), $h\omega$ is the average dissipating mode, $S = \lambda_i/h\omega$ is the vibronic coupling number, H_{el} the electronic matrix coupling element between reactants, and the other symbols have their usual signification. *Eqn. 1* shows that, in principle, four parameters can be adjusted within this model. However, this would not be very reliable to test the performance of *Eqn. 1* with so many parameters. It is usual to fit experimental data by using λ_S and H_{el} as adjustable parameters, and by fixing λ_i and $h\omega$ to typical values [6]. For the aromatic systems of *Table 1*, the values chosen were $\lambda_i = 0.1$ eV and $h\omega = 1500$ cm^{-1} [6][11].

Intersecting-State Model. The ISM is an alternative theoretical approach to the *Marcus* theory. Originally developed for reactions which involve bond-breaking bond-forming processes [12], it has also been applied to PET [8]. The fundamental assumptions of ISM are clearly opposite to those used by *Marcus*. Indeed, if the potential energy of reactants and products is also described by a parabolic curve, the reaction coordinate is now mainly governed by the inner nuclear reorganization of the two partners. Consequently, solvent plays a secondary role and does not noticeably contribute to the definition of the activation energy. The two parabolas can have different curvature, particularly if products show a large stereoelectronic change

compared to reactants. Moreover, the electron-transfer step is cooperative with the nuclear reorganization of the two partners. Thus, the molecular electronic orbitals involved in the electronic transition, in turn, indicate the chemical bonds to be considered for the whole process. The ISM, thus, has thermodynamic roots in the bond-energy-bond-order (BEBO) theory [13]. The main consequence of these conceptions is that the distance between the two parabolas (of reactants and products), which is noted d, depends on the driving force ΔG_{et} and a dynamic parameters Λ [8]. The latter represents the faculty of the two reactants at the transition state to dissipate the energy in nuclear movements. It is linked to the 'mixing entropy' of reactants' and products' states [13b]. The equations derived from all these concepts are summarized below. When reactants and products are represented by harmonic oscillators of respective strengths f_r and f_p, the crossing point that defines the transition state is the solution $x^{\ddagger}$ of *Eqn. 2* where d is the horizontal separation of the two parabolas and x is the reaction coordinate, equal to the average bond extension for the reactants. The free enthalpy of activation is then given by *Eqn. 3*.

The derivation of d leads to *Eqn. 4*.

$$\frac{1}{2}f_r x^2 = \frac{1}{2}f_p(d-x)^2 + \Delta G_{et} \tag{2}$$

$$\Delta G_{et}^{\ddagger} = \frac{1}{2}f_r(x^{\ddagger})^2 \tag{3}$$

$$d = \frac{a'(l_r^0 + l_p^0)}{2n^{\ddagger}} \ln \left[\frac{1 + \exp\left(\frac{\sqrt{2n^{\ddagger}}\Delta G_{et}}{\Lambda}\right)}{1 - \frac{1}{1 + \exp\left(\frac{\sqrt{2n^{\ddagger}}\Delta G_{et}}{\Lambda}\right)}} \right] \tag{4}$$

In *Eqn. 4*, $(l_r^0 + l_p^0)$ is the sum of the effective equilibrium bond length of reactants and products, $n^{\ddagger}$ is the total bond order of the reaction at the transition state, a' is a constant equal to 0.156, and Λ is the dynamic parameter that regulates the dissipation of the reaction free enthalpy by nonreactive modes. The value of $n^{\ddagger}$ can be calculated from bond orders of the two molecules and their conjugated radical ions [8b]. For aromatic systems pertaining to this study, the average value $n^{\ddagger} = 1.42$ can be taken for the entire set of data [8a,b]. For $(l_r^0 + l_p^0)$, the value was fixed to 250 pm [8b]. Note that it does not represent the electron-transfer distance, but the spatial extension of the two quantum boxes in which the electron moves. For oscillator strengths, reactants and products are very similar in the case of aromatic compounds, and, thus, we have fixed them both to the typical value of aromatic bonds, *i.e.*, $f_r = f_p = 300$ J mol^{-1}pm^{-2} [8]. The parameter Λ will be an adjustable parameter of the model. Once d is calculated, and the activation barrier obtained with *Eqns. 2* and *3*, the rate constant k_{et} is given by the transition-state theory under the form of *Eqn. 5*. The parameter χ is assigned to the adiabaticity of the reaction. For adiabatic PET, $\chi = 1$, and for nonadiabatic PET, it can be as low as 10^{-4}. In this study, it will be an adjustable parameter, despite the fact that

some calculation could be made [8]. However, taking Λ and χ as the two adjustable parameters of the ISM is worth to compare with the *Marcus* model, where the optimization procedure uses λ_S and H_{el}.

$$k_{et} = \frac{k_B T}{h} \chi \exp\left(-\frac{\Delta G^{\ddagger}_{et}}{RT}\right) \quad (5)$$

Table 2 collects all the fixed parameters used to adjust the *Marcus* model and ISM to the experimental data. The fitting procedure was based on a least mean-squares method. For the *Marcus* model, although λ_i and $h\omega$ were tentatively varied in reasonable ranges, no satisfying fit was obtained for the entire set of data. Thus, only the best fit pertaining to moderately exergonic reactions was retained. On the contrary, ISM was able to fit very well all the data of *Table 1*, even those at very exergonic driving force. Parameters resulting from the best fits obtained under these conditions are given in *Table 2*, and corresponding curves are shown in *Fig. 1* for the two models.

Table 2. *Resulting Parameters of Best Fits of Data Contained in* Table 1 *from the* Marcus *Model and the Intersecting-State Model*. See text for detailed procedure.

Marcus' model		Intersecting-state model	
fixed parameters	results of fit	fixed parameters	results of fit
$\lambda_i = 0.1$ eV	$H_{el} = 4 \cdot 10^{-3}$ eV	$n^{\ddagger} = 1.42$	$\chi = 0.03$
$h\omega = 1500$ cm^{-1}	$\lambda_S = 0.5$ eV	$f_r = f_p = 300$ J mol^{-1}pm^{-2}	$\Lambda = 117$ kJ mol^{-1}
		$l_r + l_p = 250$ pm	

Discussion. – *Preamble.* It appears clearly from *Fig. 1* that ISM is able to match all the data of *Table 1*, contrary to the *Marcus*' model, which describes only moderate exergonic data ($\Delta G_{et} > -1$ eV). The parameters found by the fitting procedure for ISM are physically consistent. The value $\Lambda = 117$ kJ mol^{-1} belongs to the lower limit of the typical range for this parameter (generally between 100 and 300 kJ mol^{-1} [8]). This could have been expected, since, in aromatic systems, the nuclear motions are constrained by the rigidity of the aromatic rings. As a consequence, the dissipation of excess energy at the transition state is not very efficient. The adiabatic parameter $\chi = 0.03$ gives a pre-exponential factor of $1.9 \cdot 10^{11}$ s^{-1} in *Eqn. 5*. As χ is lower than unity, PET between anthracene derivatives and aromatic donors appears to be nonadiabatic. Note that the pre-exponential term thus obtained is almost like the frequency-collisional factor usually taken to be $Z = 10^{11}$ s^{-1} in conventional kinetic schemes of electron-transfer reactions [1][14]. This fact could be an indication that PET occurs in a pure encounter complex, with no specific orientation between the two reactants. For the fit obtained with the *Marcus* theory, the values of λ_S and H_{el} lead to a maximum k_{et} of $3.5 \cdot 10^{11}$ s^{-1}, which is in good agreement with ISM. As already explained, this maximum rate constant is one order of magnitude lower than the inverse of the longitudinal relaxation time of MeCN ($1/\tau_1 = 4 \cdot 10^{12}$ s^{-1}) [5a]. Thus, the plateau observed cannot be attributed to a solvent-controlled PET. The physical meaning of this plateau is very important since it is the fundamental cause of the failure of the *Marcus* theory to account for the entire set of data of this study. More precisely, the experimental k_{et} values located in the highly exergonic region ($\Delta G_{et} < -1$ eV)

constitute the data that most strongly question the *Marcus* theory. The following discussion will be divided in two parts. First, the framework of *Marcus* will be conserved, and different hypotheses concerning the nature of the rate constant measured at highly exergonic driving force will be examined. Second, the applicability of ISM to interpret our data will be discussed, and placed within the more general context of forward PET in solution and the lack of *Marcus* inverted region.

Does Another Physical Phenomena Other Than Conventional PET Occur at Very Negative ΔG_{et}? In our previous study, the occurrence of this plateau was tentatively interpreted as a rotational effect to match a sandwich-like structure between the π-electronic clouds of the two aromatic partners. Indeed, arguments based on the *Stokes-Einstein-Debye* hydrodynamic theory brought about a rotational rate constant of $1.3 \cdot 10^{11}\ s^{-1}$ [5a]. The intrinsic rate constant of PET, thus, might be greater than those measured by the transient effect, and the kinetic might be limited by this rotation. Nevertheless, the electron-transfer distance r_{et} was measured for data obtained with the anthracene-9,10-dicarbonitrile acceptor, and it was shown that it rapidly increased from *Van der Waals* contact ($r_{et} \approx 7$ Å) to longer distance ($r_{et} = 10$ Å) [5b][15]. At such distances, the molecules freely rotate, and the orientational effect might be less restrictive. Thus, although rotational diffusion can be invoked as a limiting step within the quenching process, it still demands further experimental evidence.

Another explanation for the departure from the *Marcus* equations is frequently invoked at highly exergonic driving force: it concerns the formation of products in an excited state. Indeed, the excess of reaction free energy can be invested to produce an excited radical ion within the geminate ion pair. The difficulty for experimental evidence basically lies on the very short lifetime of this 'hot' intermediate species. This process may be involved for the data concerning anthracene-9,10-dicarbonitrile and the two benzenediamines tmbd and dmbd (see *Table 1*). In back electron transfer between geminate ion pairs, these two electron donors already showed specific features, potentially related to the possibility of forming nonrelaxed ion pairs [7]. However, the *Marcus* theory starts to depart from the experimental data at $\Delta G_{et} \approx -1$ eV, where electron donors are very conventional, and the driving force is not so negative. Furthermore, it would be a strange coincidence that the rate constant measured for tmbd and dmbd, if not involving conventional electron-transfer, correlate so well with the others by lying on the same plateau.

A third explanation would evoke a dramatic change of r_{et} with ΔG_{et}. As outlined above, r_{et} noticeably increases as ΔG_{et} becomes more negative [5a][15]. The two main influences of r_{et} on k_{et} roots on the distance dependence of H_{el} and λ_S. The former is given by *Eqn. 6*, where β is the attenuation parameter and $(r_A + r_D)$ the sum of the radii of acceptor and donor. The latter can be estimated by *Eqn. 7*, assuming a dielectric continuum model for the medium of refractive index n_{op} and static dielectric constant ε_S [11]. We have made some attempts to account for the effect of varying r_{et} on the k_{et} values given by *Eqn. 1*. Taking r_{et} as high as 15 Å did not allow to improve enough the results of *Marcus*'s calculation for data with $\Delta G_{et} < -1$ eV. If one admits that the role of r_{et} is properly described by *Eqns. 6* and *7*, the increase of distance between reactants cannot explain the discrepancy between experiments and theory.

$$H_{el}(r_{et}) = H^0_{el} \exp\left[-\frac{\beta}{2}(r_{et} - (r_A + r_D))\right] \tag{6}$$

$$\lambda_S = (e)^2 \left(\frac{1}{2r_A} + \frac{1}{2r_D} - \frac{1}{(r_A + r_D)} \right) \left(\frac{1}{n_{op}^2} - \frac{1}{\varepsilon_S} \right) \quad (7)$$

In conclusion, the whole set of data contained in *Table 1* can not be simply interpreted within the framework of the *Marcus* model. Hypothetical processes have to be invoked to rationalize data at very exergonic driving force. The lack of an experimental criterion to support one process among others lead us to confront our results with ISM, which offers an alternative theoretical approach to electron-transfer reaction.

Suitability of ISM to an Archetypal Set of k_{et} *Values.* The faculty of ISM to fit all the data of *Table 1* is particularly striking since the adjustable parameters lead to physically realistic values, as discussed above. The thermodynamic regime described by ISM with the parameters collected in *Table 2* can be better understood if the parabolas of potential energy are drawn at different values of ΔG_{et}. *Fig. 2* shows the energetic curves corresponding to the parameters given in *Table 2*, for the reactants (dashed line) and the products (full lines). The crossing points between reactants' and products' parabolas give the activation energy, and they are also indicated in *Fig. 2*. Note that reactants' and products' parabolas have the same curvature ($f_r = f_p$). For $\Delta G_{et} \geq -0.75$, the ISM and *Marcus* models are almost identical, and both describe the normal region: the activation barrier decreases as ΔG_{et} becomes more and more negative (crossing points 1, 2, and 3 in *Fig. 2*). This coincidence of the two models stems from the fact that in ISM, the separation *d* between the reactants' and products' parabolas remains nearly constant in this thermodynamic region. Indeed, $\Lambda > |\Delta G_{et}|$, and the dependence of *d* on ΔG_{et} is rather low, as seen from *Eqn. 4*. From $\Delta G_{et} = -0.75$ to -1.8 eV, the activation barrier remains at the minimum. In this range of driving force, two compensating effects occur. The decrease of ΔG_{et} would induce the appearance of a

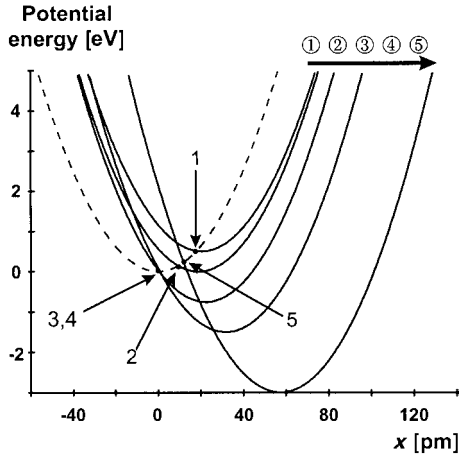

Fig. 2. *Parabolas of potential energy* vs. *bond stretching* x *for reactants* (dashed line) *and products* (plain lines ①–⑤), *calculated with the intersecting state model at different values of* ΔG_{et}: 1) *0.5 eV*, 2) *0 eV*, 3) *– 0.75 eV*, 4) *– 1.5 eV, and* 5) *– 3 eV*. Parameters used in the calculation are those given in *Table 2*. Arrows indicate the crossing points between parabola of reactants and parabolas ①–⑤ at corresponding ΔG_{et} values.

new activation barrier, due to the motion of the crossing point to the left branch of the reactants parabola. However, $|\Delta G_{et}|$ and Λ become close. Therefore, d begins to increase, which counterbalances the preceding effect. The interplay between these two phenomena implies that, actually, the crossing point remains localized near the bottom of the reactants' well (points 3 and 4 in *Fig. 2*). The barrierless regime is extended to a wide range of driving force, which strongly diverges from *Marcus* theory. Thus, the rate constants k_{et} follow a plateau, the extent of which depends on Λ and $n^{\pm}$. When ΔG_{et} is very negative (in our case, $\Delta G_{et} < -2$ eV), the increase of d overwhelms all other trends. The crossing point turns back to the right branch of the reactants' parabola (point 5 in *Fig. 2*) and brings about a new increase of activation barrier. ISM thus predicts an inverted region in k_{et}, but at very negative driving forces.

The important consequence of this thermodynamic behavior is that the plateau observed with the data of *Table 1* can find a physical interpretation without resorting to nonidentified effects. As the choice of donors and acceptors used in this study constitutes a good model and sample of typical PET between aromatic molecules, it is interesting to notice the suitability of the ISM to account for all the intrinsic rate constants k_{et}. The authors of the ISM have already applied their model with some significant success to the problematic PET [8][16]. For instance, ISM can fit with success the totality of the bimolecular quenching rate constants measured by *Rehm* and *Weller* [8b]. It can also be applied to the back electron transfer within geminate ion pairs, since ISM also predicts an inverted region [8c]. The only parameter really required to adjust is Λ, and it controls the global kinetic behavior towards ΔG_{et}. To the best of our knowledge, this is the first time that the challenge between the ISM and *Marcus* models is so clearly shown directly on forward PET *intrinsic* rate constants k_{et}. The use of k_{et} has allowed to rule out some hypotheses that have been generally invoked when diffusion could mar the actual process. It obviously questions the validity of the main conception of the *Marcus* theory, namely the preponderant role of solvent reorganization on the definition of reaction coordinate, and then on the activation barrier. Nevertheless, even though the data examined in this study can be considered as archetypal in PET, definitive conclusions should not be drawn heedlessly.

Conclusion. – The use of the intersecting state model (ISM) has brought about new insights into the interpretation of the plateau followed by the intrinsic rate constants k_{et} of PET between excited anthracene derivatives and aromatic electron donors. In the framework of ISM, this plateau is entirely described by the fitting procedure with physically realistic parameters. On the contrary, to apply the *Marcus* theory to the whole set of data requires application of some processes, such as excited-products formation, that still remain hypothetical. This challenge between two theoretical models pertains to a pragmatic point of view. It aims at questioning the applicability of two available antagonistic theories by confronting them to prototypal experimental data in PET. The fact that the *Marcus* theory is widely accepted should not lead one to consider it as a dogma: in forward bimolecular PET, it has long been recognized that some discrepancies remain, which may require new theoretical approaches to be understood. Undoubtedly, this attitude, in combination with the well-identified successes of the *Marcus* theory in many domains, would enrich our global comprehension of PET.

The authors wish to thank Dr. *Luis Arnaut* for his very valuable comments concerning some points of the intersecting-state model.

REFERENCES

[1] D. Rehm, A. Weller, *Isr. J. Chem*. **1970**, *8*, 259.
[2] D. Peak, T. C. Werner, R. M. Dennin Jr., J. K. Baird, *J. Chem. Phys*. **1983**, *79*, 3328; J. Keizer, *J. Am. Chem. Soc*. **1983**, *105*, 1494.
[3] S. Murata, M. Tachiya, *J. Phys. Chem*. **1996**, *100*, 4064; S. Murata, M. Nishimura, S. Y. Matsuzaki, M. Tachiya, *Chem. Phys. Lett*. **1994**, *219*, 200.
[4] B. Stevens, C. J. Biver III, *Chem. Phys. Lett*. **1994**, *226*, 268; B. Stevens, C. J. Biver III, D. N. McKeithan, *Chem. Phys. Lett*. **1991**, *187*, 590.
[5] a) X. Allonas, P. Jacques, *Chem. Phys*. **1997**, *215*, 371; b) P. Jacques, X. Allonas, *Chem. Phys. Lett*. **1995**, *233*, 533.
[6] I. R. Gould, D. Ege, J. E. Moser, S. Farid, *J. Am. Chem. Soc*. **1990**, *112*, 4290.
[7] E. Vauthey, *J. Phys. Chem. A* **2001**, *105*, 340.
[8] a) C. Serpa, L. G. Arnaut, *J. Phys. Chem. A* **2000**, *104*, 11075; b) S. J. Formosinho, L. G. Arnaut, R. Fausto, *Prog. React. Kinet*. **1998**, *23*, 1; c) L. G. Arnaut, S. J. Formosinho, *J. Mol. Struct. (THEOCHEM)* **1991**, *233*, 209.
[9] M. A. Smitha, E. Prasad, K. R. Gopidas, *J. Am. Chem. Soc*. **2001**, *123*, 1159; C. Turro, J. M. Zaleski, Y. M. Karabatsos, D. G. Nocera, *J. Am. Chem. Soc*. **1996**, *118*, 6060; J. M. Chen, T.-I. Ho, C.-Y. Mou, *J. Phys. Chem*. **1990**, *94*, 2889; C. Creutz, N. Sutin, *J. Am. Chem. Soc*. **1977**, *99*, 241.
[10] P. Jacques, D. Burget, X. Allonas, *New J. Chem*. **1996**, *20*, 933.
[11] a) R. A. Marcus, N. Sutin, *Biochim. Biophys. Acta* **1985**, *811*, 265; b) R. A. Marcus, *J. Chem. Phys*. **1956**, *24*, 966.
[12] A. J. C. Varandas, S. J. Formosinho, *J. Chem. Soc., Faraday Trans. 2* **1986**, *82*, 953.
[13] a) H.-S. Johnston, C. Parr, *J. Am. Chem. Soc*. **1963**, *85*, 2544; b) N. Agmon, R. D. Levine, *Chem. Phys. Lett*. **1977**, *52*, 197.
[14] R. A. Marcus, *Int. J. Chem. Kinet*. **1981**, *13*, 865; R. A. Marcus, *J. Chem. Phys*. **1965**, *43*, 2654.
[15] T. N. Inada, C. S. Miyazawa, K. Kikuchi, M. Yamauchi, T. Nagata, Y. Takahashi, H. Ikeda, T. Miyashi, *J. Am. Chem. Soc*. **1993**, *121*, 7211.
[16] L. G. Arnaut, S. J. Formosinho, *J. Photochem. Photobiol. A: Chem*. **1997**, *111*, 111; S. J. Formosinho, L. G. Arnaut, *J. Photochem. Photobiol. A: Chem*. **1994**, *82*, 11.

Received June 9, 2001